Role of diffusion in scaling of polymer chain aggregates found in vapor deposition polymerization

Sairam Tangirala and D. P. Landau

Role of Diffusion in Scaling of Polymer Chain Aggregates Found in Vapor Deposition Polymerization

Sairam Tangirala* and D.P. Landau

Center for Simulational Physics, The University of Georgia, Athens, GA 30602.

Polymer chain aggregates grown by 1+1D Monte Carlo simulations of vapor deposition polymerization (VDP) were studied. The dynamic scaling behavior of polymer chain length distribution $n_s(t)$ was studied as a function of chain length (s), deposition time (t), and the ratio $G = D/F$ of deposition rate (F) and free monomer diffusion (D). The dynamic scaling approach was employed to highlight the dependence of $n_s(t)$ on t, s, and G. With an increase in t, we found a power law increase in $n_s(t)$ and total number of polymer chains $N_{total}(t)$, given by, $N_{total}(t) \sim t^\omega$ and $n_s(t) \sim t^\omega$ with exponent $\omega = 1.01(2)$ that was invariant for a range of $G = 10$ to 10^4. For small s and $t = 10^3$, 5×10^3, and 10^4, $n_s(t)$ decreased according to $n_s(t) \sim s^{-\tau}$ with $\tau = 0.58(2)$. As G was increased from 10 to 10^4, we observed a systematic influence of G on the rescaled $n_s(t)$ data that prevented the manifestation of unique scaling function for polymer chain aggregates. The dependence of scaling functions of $n_s(t)$ on G elucidates the sensitivity of polymer chain aggregates to G and is thought to be a characteristic of VDP.

PACS numbers: 81.15.Aa, 68.55.-a, 81.15.Gh, 82.35.-x, 07.05.Tp

I. INTRODUCTION

Vapor deposition polymerization (VDP) refers to the growth of higher molecular weight products directly from lower molecular weight gas precursors. Inside a reactor, the precursors undergo polymerization reaction to form immobilized films on the desired substrate. Films can be grown to desired thicknesses precisely, enabling ultrathin, pinhole-free coatings, and materials can be deposited even onto rough surfaces and complex geometries yielding conformal coatings. [1]. In a typical VDP experiment, a wafer (2D substrate) is exposed to one or more gas phase precursors that produce free monomers which impinge on the substrate at random locations and react to produce the desired deposit on the substrate.

The advantages of vapor-based polymerization methods is their versatility in synthesizing both simple and complex polymers with relative ease and at generally low temperatures along with control of the composition and architecture of the resulting materials. Other benefits include high accuracy, solvent-free environments, excellent adhesion, high coating fidelity, the use of solvent-free processes, and the ability to accommodate custom-tailored surface modifications [2, 3]. Many experimental efforts have focussed on the formation of polymer thin films using VDP [4–6] as this technique has immense technological applications in microelectronic interconnects [7, 8], organic electronics [8], and biomedical applications [9]. The performances of devices based on VDP, depend not only on the precursor material, but also on the arrangement of its molecules in the films [10]. To investigate the film growth, various kinetic processes should be considered at molecular scales, including the interlayer material transport that determine the film properties. For devel-oping an effective method of growing organic nanostructures and for their success in various applications, the control over parameters like diameter, length, and morphology is very important . The morphology and size control is of critical importance in the synthesis of the organic nanostructures and can directly determine the performances of the devices based on them.

Although vapor transfer [11–14] is a popular method used to grow organic nanostructures, literature on the size controllable growth of the nanostructures is very limited. Many recent studies [15–19] have focused on the behavior of overall polymer films properties like film density, interface width, end-to-end distance, etc. However, there is a very limited understanding of the aggregation process of polymer chains themselves apart from literature on submonolayer studies of VDP [16] that reported the existence of three distinct growth regimes: initiation (I), chain propagation (P), and saturation regime (S) and the recent experimental work on island nucleation during VDP [20] that indicates a new type of surface growth governed by reaction-limited aggregation in the films grown by VDP. The mechanism of polymer film growth by VDP is quite different from that of conventional physical vapor deposition. Polymer film growth involves monomer reaction in the bulk of the film, which needs to be considered in growth models of VDP [21]. Although it is quite important to understand the aggregation mechanism on the molecular level, such an understanding is quite poor in polymerization driven processes as compared to those of metals and semiconductors. In this communication, we exlpore this niche and provide an impetus in understanding the physics governing polymer aggregation based growth systems.

---
*Electronic address: sairam@hal.physast.uga.edu
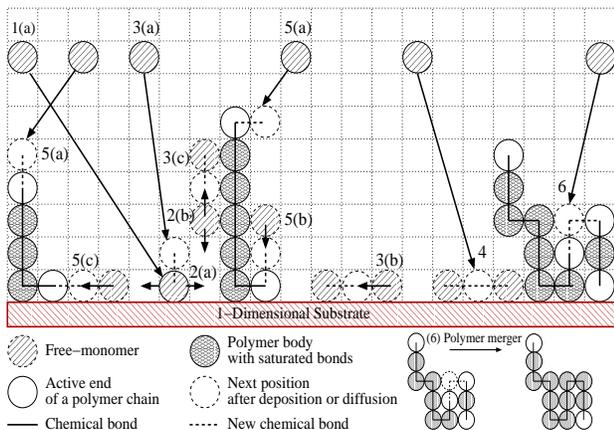
FIG. 1: (Color online) Schematic of our 1+1D growth model. Various processes implemented in our model are explained using following labels; 1(a): free monomer deposition at random angles. 2(a,b): Adsorbed free monomer diffuses on the substrate and a polymer chain respectively. 3(a), 4: Polymer chain initiation resulting from random angle deposition. 3(b,c): Chain initiation resulting from free monomer diffusion on the substrate and polymer chain respectively. 5(a): Chain propagation resulting from free monomer deposition onto the active end of a polymer chain; 5(b,c) Chain propagation due to free monomer diffusion on polymer chain and substrate respectively. 6: Polymer merger resulting from deposition. In all processes, the straight lines with arrows represent the trajectory of free monomers.

II. MODEL AND METHOD

A $1 + 1D$ lattice model similar to the one employed earlier [15, 17, 18] was used in our study of polymer chain aggregates. In our computational model, a number of Monte Carlo moves were employed to simulate various dynamical processes occurring during the VDP growth. Figure 1 summarizes the processes occurring during the non-equilibrium growth on a $1D$ substrate of length L with periodic boundary conditions. Process 1(a) shows gas phase free monomers depositing onto the substrate at random locations with uniform launch angle distribution. We neglected the reemission effects and the impinging free monomers are assumed to always stick to the nearest neighboring particle that comes on its deposition path. The free monomers may get adsorbed either on the substrate (shown by process 2(a)) or on the polymer chains (process 2(b)). Adsorbed free monomers can diffuse along the adsorbent to any of the nearest-neighboring unoccupied sites with equal probability. The polymer chain length s refers to the number of monomers forming a polymer chain. When an impinging free monomer encounters another free monomer on the substrate as its nearest neighbor (process 3(a)), both are frozen and undergo a chemical reaction to form a dimer ($s = 2$). Dimers can also be formed due to free monomer diffusion on substrate (process 3(b)) or existing polymer chains (process 3(c)). Polymers with $s = 3$

can also be formed after deposition (process 4). When an impinging free monomer encounters an active end of a polymer chain, it attaches itself to the chain and increases s by one unit (process 5(a)). A diffusing free monomer can meet an active end of a chain in its neighborhood and get bonded to that polymer chain (processes 5(b), 5(c)). In linear polymer system studied here, the free monomers are allowed to form a maximum of two chemical bonds; and, at any given time, only the two ends of the polymer chain are chemically active, resulting in the chain propagation at these two end locations only. The chain portion (of the polymer), excluding the two chemically active ends, is not allowed to form chemical bonds with neighboring free monomers. Free monomers can, however, be physically adsorbed on the chain and can diffuse along the chain (processes 2(b), 5(b)). *Polymer-merger* occurs during the growth when the active ends of two different polymers meet as nearest neighbors (process 6) and react chemically to join the two polymers into one longer polymer chain with higher molecular weight. The resulting polymer chain is left with two active-ends, one from each of the parent polymers. When ever a free monomer was the nearest neighbor to the active ends of more than two polymers, we selected a random pair of polymers and performed polymer-merger. In the case when both the active-ends belonging to the same chain appear as nearest neighbors, a chemical bond between the ends is prohibited.

All simulations start with an empty 1D substrate and at each stage of the simulation, either a deposition or a diffusion step is performed with probabilities p_F and p_D according to Ref. [22],

$$p_F = \frac{1}{[1 + N_1 G]}, \quad p_D (= 1 - p_F) = \frac{N_1 G}{[1 + N_1 G]}, \quad (1)$$

where N_1 is the number of free monomers in the system. The incoming free monomer flux F was fixed for different D and an increase in D was parametrized as an increase in the ratio $G(= D/F)$. In our model, MC time unit $t = 1$ corresponded to the deposition of L free monomers in the system. Throughout the simulations the lists of all free monomers, active-ends, and polymer chains were continually updated. We used the KISS random number generator [27] to make all stochastic decisions during the VDP growth. We also tested our program with the standard ISO C random number function included in the GNU library. The results from both random number generators were found to be identical to within statistical errors. The statistical errors of the data shown in included plots were calculated from 500 independent simulations and were smaller than the symbol sizes. We tested our simulations using $L = 200, 300, 400,$ and 500 and for presenting results in this paper, we chose $L = 200$ as a representative substrate length and performed simulations until $t = 10^4$ for varying values of G.
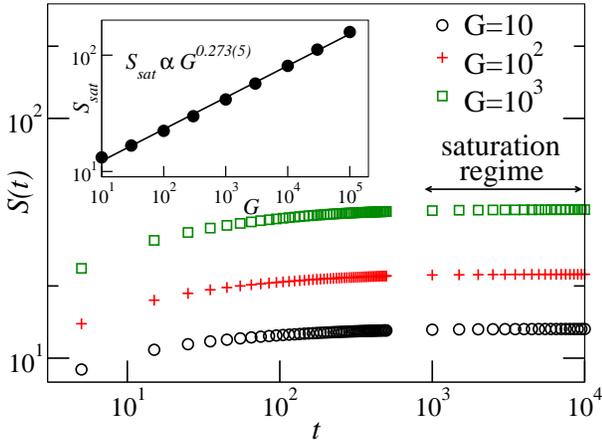
FIG. 2: (Color online) The mean chain length $S(t)$ as a function of t for $L = 200$ and $G = 10$, 10^2, and 10^3. The indicated saturation regime is characterized by a nearly constant $S(t)$ and demonstrates a steady state VDP growth. The inset shows the variation of mean chain length in saturation regime (S_{sat}) with G. A straight line fit of the inset log-log plot indicates a power law increase of S_{sat} with G, the error in the exponent was obtained from the curve fit.

FIG. 3: (Color online) Plots of polymer chain length distribution $n_s(t)$ as a function of s for $L = 200$ and $G = 10$ at $t = 10^3$, 5×10^3, and 10^4. The straight lines have a slope $\tau \approx -0.58(2)$ and indicate a power-law dependence of $n_s(t)$ on s. The error in the exponent was obtained from the curve fit.

III. RESULTS

A quantity commonly used to characterize polymer chain length is the average linearized chain length $S(t)$ defined as the first moment of $n_s(t)$ [22],

$$S(t) = \frac{\sum_{s>1} n_s(t)s}{\sum_{s>1} n_s(t)}. \qquad (2)$$

Figure 2 shows the variation of $S(t)$ for $G = 10$, 10^2, and 10^3. With an increase in t from 0 to 10^4 and for indicated G, the $S(t)$ was observed to increase at lower t and attain an asymptotic value for larger t denoted by S_{sat}. The presence of a nearly constant S_{sat} for $t \geqslant 1000$ indicates a steady-state saturation regime during VDP, as indicated in Fig. 2. As G was increased from 10 to 10^5, we observed a power-law increase in S_{sat} given by, $S_{sat} \propto G^{0.273(5)}$ as shown in the inset of Fig. 2. In the following sections we discuss the scaling of polymer chain aggregates in the steady state region (saturated regime) of VDP growth.

A widely used method for the description of growing aggregates (clusters) is the determination of distribution function of aggregates, which, in the studies of polymers, is referred to as the polymer chain length distribution function $n_s(t) = N_s(t)/L$, where $N_s(t)$ is the number of clusters containing s monomers at time t [22–24]. In general, any diffusion bias inherent in the aggregate growth leads to scaling behavior of $n_s(t)$; and if diffusion were independent of s, a diffusive-like kinetic universality class is manifested [25].

Figure 3 shows the variation of $n_s(t)$ as a function of s for $t = 10^3$, 5×10^3, 10^4 (within saturation regime), and $G = 10$. For studied t, the $n_s(t)$ distribution de-

creased to zero for increasing chain lengths s. Similar behavior was observed for a range of G varying from 10 to 10^4. For a fixed G and increasing t, the smaller chains do not vanish by merging (to larger chains) and instead continue to increase in number throughout the growth process. As seen in Fig. 3, for all s, an increase in t from 10^3 to 10^4 merely increases the numerical value of $n_s(t)$ without much effecting the length of the largest polymer chains present in the simulations. The critical value of s at which power-law decay cuts off does not vary much with an increase in t and this behavior is thought to be specific to VDP unlike conventional growth studies of diffusion-limited cluster aggregation and reaction-limited cluster aggregation studied in Refs. [22, 23, 26]. In Fig. 3, the data for small s gives information about the growth of larger polymer aggregates from smaller chains via polymerization process. For small s, we observed a straight line behavior on the log-log plots of Fig. 3 that corresponded to a power-law decay of $n_s(t)$,

$$n_s(t) \sim s^{-\tau}, \qquad (3)$$

with an average $\tau = 0.58(2)$ for indicated t. The exponent τ was found to be invariant with an increase in G from 10 to 10^4.

For $G = 10$, the Fig. 4 shows an increase in $n_s(t)$ with an increase in t for representative chains with length $s = 10$, 20, 40, and 50. For indicated s, the $n_s(t)$ distribution was observed to follow a power-law

$$n_s(t) \sim t^\omega, \qquad (4)$$

with an average exponent $\omega = 1.01(2)$ that can be used to quantify the growth rate of $n_s(t)$. The power-law dependence of $n_s(t)$ on t observed in the main plot of Fig. 4 explains the presence of smaller chains throughout the VDP growth process (seen earlier in Fig. 3) and indicates that the smaller polymer chains do not have the
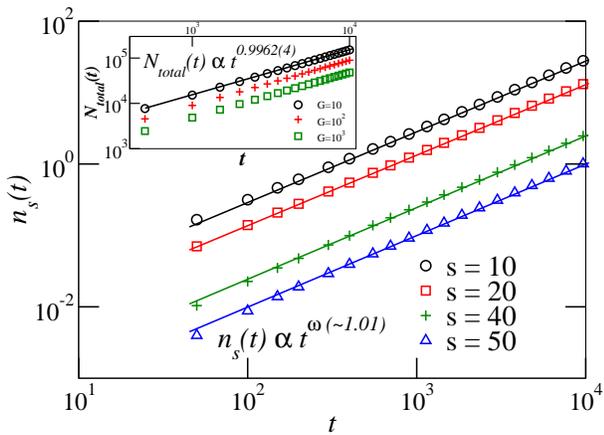
FIG. 4: (Color online) Plots of chain length distribution $n_s(t)$ as a function of t for $L = 200$, $G = 10$, and selected chain lengths $s = 10, 20, 40,$ and 50. The straight lines have a slope $\omega \approx 1.01(2)$ and indicate a power law increase of $n_s(t)$ with t. The inset shows a power law increase in total number of polymer chains N_{total} with t, its exponent was found to be same as ω (within error bars). The error in ω was obtained
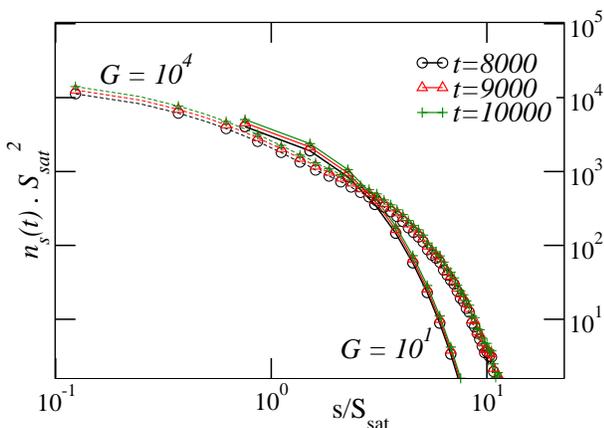
FIG. 5: (Color online) Comparison of scaled chain length distributions for $L = 200$ and $G = 10$ and 10^4. For a given G and $t = 8 \times 10^3$, 9×10^3, and 10^4 the rescaled plots collapse onto a single scaling function. However, a variation in G affects the behavior of scaling functions of $n_s(t)$ and produces non-overlapping curves at varying G. The connecting lines are guide for the eyes.

tendency to merge and form larger chains inspite of the polymer-merger move implemented in the simulations. In the inset of Fig. 4, we show the total number of polymer chains $N_{total}(t)$ in the system as a function of t. Here too, we observed a power-law increase in $N_{total}(t)$ with t given by, $N_{total}(t) \propto t^{0.9962(4)}$ that corroborated our finding of power-law increase in $n_s(t)$ seen in main plot of Fig. 4.

From the behavior of $n_s(t)$ in Eqns. (3), (4), and

using the theory of dynamic scaling for cluster aggregation employed in [20, 22], we plot the rescaled quantity $(n_s(t)S_{sat}^2)$ versus s/S_{sat} in Fig. 5 for $t = 8 \times 10^3$, 9×10^3, 10^4, and $G = 10, 10^4$. For a given G, the aforementioned rescaling shifts $n_s(t)$ shown in Fig. 3 such that all data points for varying t and s collapse onto a single curve, commonly referred to as the *scaling function*. The scaling functions obtained for $G = 10$ and 10^4 (shown in Fig. 5) are observed to decrease monotonically, a similar behavior was reported in a recent experimental work on VDP [20] where authors noticed a power law scaling of island densitiy distribution in the large island regime $((s/S_{sat}) \geq 1)$. We note that the scaling functions of Fig. 5 are different from the conventionally studied monomodal (bell-shaped) curves obtained in atomistic growth models [22, 24]. This characteristic behavior of scaling functions is probably due to the accumulation of polymer chains (of all sizes) resulting in a diverging $n_s(t)$ as a function of t (see Fig. 4). Since the polymer chain growth is via propagation or polymer-merger through the active-ends, the temporal evolution of $n_s(t)$ strongly depends on the chemical binding nature of the precursors involved in VDP. The complicated screening action resulting from a limited bonding nature of free monomer can be considered to bring about a significant modification to the aggregation mechanism.

In Fig. 5 we note that the scaling functions corresponding to $G = 10$ and 10^4 do not collapse onto a unique master curve. We thus note that G is an important parameter in determining the scaling of polymer chain aggregates. We hope that our observation of non-overlapping scaling functions merits itself additional new studies on understanding the change in the aggregation mechanism brought about by G.

IV. CONCLUSIONS

In summary, a 1+1D Monte Carlo VDP growth model was used to study the role of $G = D/F$ in determining the dynamic scaling of polymer chain distribution function $n_s(t)$. The scaling functions characterizing polymer chain aggregates were found to be monotonically decreasing and noticably different from those of diffusion mediated systems. The ratio G was seen to have a strong influence on determining the scaling functions that characterize the aggregation process in VDP.

V. ACKNOWLEDGEMENTS

[1] M. Anthamatten and K. K. S. Lau, *Encyclopedia of Chemical Processing* (Taylor & Francis, 2009).

[2] J. Lahann, Polymer International **55**, 1361 (2006).

[3] S. Rogojevic, J. A. Moore, and W. N. Gill, Journal of Vacuum Science & Technology A **17**, 266 (1999).

[4] G. W. Collins, S. A. Letts, E. M. Fearon, R. L. McEachern, and T. P. Bernat, Phys. Rev. Lett. **73**, 708 (1994).

[5] F. Biscarini, P. Samor'i, O. Greco, and R. Zamboni, Phys. Rev. Lett. **78**, 2389 (1997).

[6] J. Fortin and T. Lu, Chemistry of Materials **14**, 1945 (2002).

[7] T.-M. Lu and J. A. Moore, Mater. Res. Soc. Bull **20**, 28 and references therein (1997).

[8] C. P. Wong, *Polymers for Electronic and Photonic Application* (Academic Press, Boston, MA, 1993).

[9] J. Lahann, Polymer International **55**, 1361 (2006).

[10] D. Y. Zhong, M. Hirtz, W. C. Wang, R. F. Dou, L. F. Chi, and H. Fuchs, Phys. Rev. B **77**, 113404 (2008).

[11] S. Liu, J. B. H. Tok, J. Locklin, and Z. Bao, Small **2**, 1448 (2006).

[12] Q. Tang, H. Li, M. He, W. Hu, C. Liu, K. Chen, C. Wang, Y. Liu, and D. Zhu, Advanced Materials **18**, 65 (2006).

[13] Q. Tang, H. Li, Y. Song, W. Xu, W. Hu, L. Jiang, Y. Liu, X. Wang, and D. Zhu, Advanced Materials **18**, 3010+ (2006).

[14] Q. Tang, H. Li, Y. Liu, and W. Hu, Journal of the American Chemical Society **128**, 14634 (2006).

[15] W. Bowie and Y. P. Zhao, Surface Science **563**, L245 (2004).

[16] Y.-P. Zhao, A. R. Hopper, G.-C. Wang, and T.-M. Lu, Phys. Rev. E **60**, 4310 (1999).

[17] S. Tangirala, D. P. Landau, and Y.-P. Zhao, Phys. Rev. E **81**, 011605 (2010).

[18] S.-W. Son, M. Ha, and H. Jeong, Journal of Statistical Mechanics - Theory and Experiment (2009).

[19] I. J. Lee, M. Yun, S.-M. Lee, and J.-Y. Kim, Phys. Rev. B **78**, 115427 (2008).

[20] I. Lee and M. Yun, Macromolecules **43**, 5450 (2010).

[21] S. Ganguli, H. Agrawal, B. Wang, J. F. McDonald, T. M. Lu, G.-R. Yang, and W. N. Gill, Journal of Vacuum Science and Technology: A **15**, 3138 (1997).

[22] J. G. Amar, F. Family, and P.-M. Lam, Phys. Rev. B **50**, 8781 (1994).

[23] T. Vicsek and F. Family, Phys. Rev. Lett. **52**, 1669 (1984).

[24] M. C. Bartelt and J. W. Evans, Phys. Rev. B **46**, 12675 (1992).

[25] F. Leyvraz and S. Redner, Phys. Rev. Lett. **88**, 068301 (2002).

[26] A. Moncho-Jordá, F. Martínez-López, and R. Hidalgo-Álvarez, Physica A: Statistical Mechanics and its Applications **282**, 50 (2000).

[27] G. Marsaglia, J. Mod. Appl. Statist. Methods **2**, 2 (2003).